Icarus **146**, 263–269 (2000)
doi:10.1006/icar.2000.6383, available online at http://www.idealibrary.com on IDEAL®

Theoretical Modeling of the C_2 Fluorescence Spectrum in Comet Hale-Bopp[1]

P. Rousselot

Observatoire de Besançon, B.P. 1615, 25010 Besançon Cedex, France
E-mail: philippe@obs-besancon.fr

S. M. Hill,[2] M. H. Burger, and D. A. Brain

University of Colorado, Campus Box 391, Boulder, Colorado 80309-0391

and

C. Laffont and G. Moreels

Observatoire de Besançon, B.P. 1615, 25010 Besançon Cedex, France

Received December 14, 1998; revised February 5, 2000

We report on observations and analysis of the C_2 Swan band $\Delta v = 0$ sequence in the optical spectrum of Comet Hale-Bopp. One set of observational data was obtained when this comet was at a large heliocentric distance (3.03 AU). This unusual distance provided the opportunity to enhance our knowledge of the intercombination transitions in C_2.

These transitions are forbidden for electric dipole radiation, but they exist due to higher order multipole radiation. Although the transition probabilities are several orders of magnitude smaller than allowed electronic transitions, the intercombination bands play a key role in the fluorescence process of the C_2 radical. This role is to provide a cooling path for rotational and vibrational populations seen in the visible spectrum. Because their exact transition probability is not yet completely clear, better quantitative knowledge of these transitions can help constrain C_2 quantities in comets.

To analyze the data, an equilibrium fluorescence model with 5652 different vibrational levels was created. This model included the triplet and singlet systems of C_2 involved in the fluorescence process. Theoretical spectra corresponding to different values of the electronic transition moments for the $a^3\Pi_u$–$X^1\Sigma_g^+$ and $c^3\Sigma_u^+$–$X^1\Sigma_g^+$ transitions were computed. These spectra were then compared to the observational data. A good fit is obtained for transition moments of $5 \times 10^{-6} \leq |D_{a-X}|^2 = |D_{c-X}|^2 \leq 10^{-5}$ atomic units (a.u.), for spectra obtained far from the nucleus where the fluorescent equilibrium is reached.

Key Words: **comets; comet, Hale-Bopp; spectroscopy; C_2.**

1. INTRODUCTION

The C_2 molecule is a well-known species in the cometary spectra, with one of the brightest emissions in the visible spectrum. Analysis of this radical in comets has shown that excited vibration–rotation levels are highly populated. This is due to the homonuclear nature of this molecule, which implies that it has no permanent electric dipole moment. Consequently, electric dipole transitions among vibrational or rotational levels within an electronic state are forbidden. This prevents cooling of the excited populations by radiation.

The Swan system $d^3\Pi_g$–$X^1\Sigma_g^+$ is responsible for the bright emission bands appearing around 5000 Å. If this system existed in isolation, with no interactions with other electronic states, one would expect to observe a Boltzmann distribution of the level populations having a temperature close to the color temperature of the Sun (i.e., $T \simeq 5800$ K). This temperature is not observed, and several authors have shown that it is necessary to take into account transitions involving other electronic states.

The study of the energy levels of the C_2 radical reveals that both singlet states ($X^1\Sigma_g^+$, $A^1\Pi_u$, $C^1\Pi_g$, $D^1\Sigma_u^+ \ldots$) and triplet states ($a^3\Pi_u$, $b^3\Sigma_g^-$, $c^3\Sigma_u^+$, $d^3\Pi_g$, $e^3\Pi_g \ldots$) exist. Gredel *et al.* (1989) have shown that the spectrum of the C_2 radical can be effectively modeled by considering the first six electronic states ($X^1\Sigma_g^+$, $a^3\Pi_u$, $b^3\Sigma_g^-$, $A^1\Pi_u$, $c^3\Sigma_u^+$, and $d^3\Pi_g$) and the six transitions occurring between them. These authors have also carefully studied the influence of the two intercombination transitions parameters ($a^3\Pi_u$–$X^1\Sigma_g^+$ and $c^3\Sigma_u^+$–$X^1\Sigma_g^+$). These singlet–triplet transitions are forbidden in electric dipole radiation, but they proceed by higher order multipole radiation. The corresponding transition probabilities are several orders of

[1] Based on observations collected at the European Southern Observatory, Chile (proposal ID: 60.F-0309).

[2] Current affiliation: NOAO, Space Environment Center, 325 Broadway, Boulder, CO 80303.

0019-1035/00 $35.00

magnitude smaller than the other electronic transitions. Nevertheless, the intercombination bands play a key role in understanding fluorescence processes in the C_2 molecule.

These intercombination transitions "cool down" the rotational and vibrational Boltzmann temperatures of the C_2 radicals. This cooling is effectively what pure vibrational and/or rotational transitions would provide were they allowed.

Steady-state cometary C_2 fluorescence is governed by competition between production and loss of excited states. Production is due to absorption of photons from the solar radiation field. Loss occurs by spontaneous emission occurring first between excited and ground electronic states (either $X^1\Sigma_g^+$ or $a^3\Pi_u$) and second between the two ground electronic states. This leads to de-excitation of the different vibrational and/or rotational levels.

Thus, accurate modeling of the C_2 emission spectrum in comets requires the best possible quantitative knowledge of the intercombination transitions. The transition occurring between the two ground electronic states is especially important.

This intercombination system has yet to be observed directly (Rousselot *et al.* 1998). However, it has been studied theoretically (e.g., Le Bourlot and Roueff 1986) and by comparison between the observed Swan bands and the computed fluorescent spectrum taking into account this system (A'Hearn and Feldman 1980, Lambert and Danks 1983, Krishna Swamy and O'Dell 1987, O'Dell *et al.* 1988, Gredel *et al.* 1989, Rousselot *et al.* 1994).

Gredel *et al.* (1989) conducted an extensive study of the C_2 emission spectrum by varying the electronic transition moments for the $a^3\Pi_u$–$X^1\Sigma_g^+$ and $c^3\Sigma_u^+$–$X^1\Sigma_g^+$ transitions ($|D_{a-X}|^2$ and $|D_{c-X}|^2$). They attempted to explain high-resolution spectra taken on Comet Halley by using $|D_{a-X}|^2 = |D_{c-X}|^2 = 3.5 \times 10^{-6}$ a.u. Their model seemed to give acceptable results for spectra obtained far from the nucleus. For spectra obtained on the nucleus, it was necessary to use the improbable dilution factor of 2.25 for the solar spectrum.

Subsequent to Gredel *et al.* (1989), Rousselot *et al.* (1994) showed that the C_2 emission spectrum takes a long time to reach fluorescence equilibrium. Thus, near-nuclear spectra cannot be explained by equilibrium models. In fact, even the "coma spectrum" used by Gredel *et al.* may not have reached equilibrium.

Heliocentric distance is an important parameter in the investigation of the intercombination transitions. For a given value of the intercombination transition moments, the excitation temperatures (rotational and vibrational) are dependant on the solar flux received by the comet. In a rough approximation we can say that the influence of the "cooling" due to the intercombination transitions is more important, compared to the "heating" due to the solar flux, when the heliocentric distance is large. Comet Hale-Bopp was one of the most active comets observed since the advent of modern astronomical spectroscopic studies. It constituted a good opportunity to improve knowledge of the C_2 fluorescence process because it was possible to obtain spectra with a good S/N ratio even far from the Sun.

2. OBSERVATIONAL DATA

The observational data set was obtained when Comet Hale-Bopp was at a large heliocentric distance, on October 12, 1997, at the European Southern Observatory (La Silla, Chile) with a 1.52-m telescope and a Boller and Chivens spectrograph. Five different spectra of Comet Hale-Bopp were obtained with an integration time of 10 mn each. These spectra were obtained with a slit oriented along the north–south direction, i.e., in a direction roughly perpendicular to the tail axis. At this time the geocentric distance of Hale-Bopp was $\Delta = 3.15$ AU, the heliocentric distance was $R = 3.03$ AU, and the heliocentric velocity was $v_c = +20$ km/s.

The spatial scale of the spectra is 0.82 arcsec/pixel. With a spectral scale of 0.981 Å/pixel and a slit width corresponding to 1.64 arcsec, the spectral resolution obtained is 2 Å. The CCD used was a 2048×2048 array of 15-μm pixels, giving a spectral range from about 4160 Å to about 6170 Å. The spatial scale corresponds to 1872 km/pixel in the Comet Hale-Bopp coma.

All images were bias-subtracted and divided by a normalized flat-field. The flat-field was taken by using a flat screen inside the dome, lit by a tungsten lamp. Wavelength calibration was done using calibration spectra obtained with an internal helium and argon lamp. No significant change concerning the wavelength calibration was noticed for the different spectra. This calibration was done with a 2-D algorithm taking into account the small curvature in the spatial direction. The spectra were corrected for the atmospheric extinction and calibrated in absolute units (erg/cm^2/s/Å) using the spectra of two standard stars.

The solar continuum was subtracted by using a theoretical solar spectrum convolved with an instrument response function. The slope of this solar spectrum was adjusted to the cometary spectra by using two spectral regions where no molecular emission lines were apparent (4880–4920 Å and 5180–5220 Å).

3. THE MODEL

To maximize information about the C_2 intercombination transitions, we limited the number of free parameters. The key constraint was to study only the spectra obtained far from the nucleus where the fluorescent equilibrium is reached. This allows the spectra to be compared with a steady-state model.

The spectra obtained close to the nucleus present a better signal-to-noise ratio, but they are far from the fluorescent equilibrium (Rousselot *et al.* 1994, 1995, Laffont *et al.* 1998). Modeling such spectra would imply other free parameters, such as the initial energy distribution due to the photodissociation process of the C_2 parent-molecule or the time elapsed from the photodissociation for the different C_2 molecules encountered along the line of sight. The goal of this work (the improvement of the quantitative knowledge of the electronic intercombination transition moments) could then hardly be achieved.

From a theoretical point of view, it is easier to consider fluorescent equilibrium rather than to include an initial energy

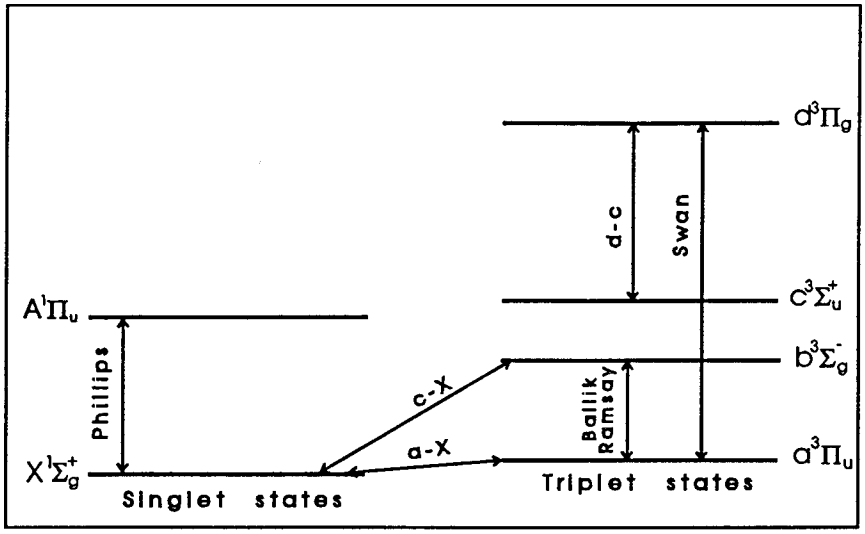

FIG. 1. Energy level diagram of the C_2 molecule. Each energy level corresponds to the first vibrational state of the respective electronic state. Note that the vibrational levels of the $X^1\Sigma_g^+$ and $a^3\Pi_u$ states are "mixed"; i.e., they cover the same range of energy values. An excited C_2 radical in any vibrational level of these two electronic states (except the lowest $X^1\Sigma_g^+$ vibrational level) can decay to vibrational states of the other ground electronic state. The electronic transitions represented here are the transitions taken into account in our model.

distribution and an elapsed time. Zucconi and Festou (1985) present the matrix formulae needed for this type of calculation. We used this formalism to determine relative ground state populations of C_2 molecules at equilibrium (see below).

We considered all C_2 energy levels corresponding to rotational quantum numbers $N \leq 90$ and vibrational quantum numbers $v \leq 5$ within the first six electronic states (i.e., $X^1\Sigma_g^+$, $a^3\Pi_u$, $b^3\Sigma_g^-$, $A^1\Pi_u$, $c^3\Sigma_u^+$, and $d^3\Pi_g$). The total number of levels considered was 5652.

The electronic transitions considered are Phillips ($A^1\Pi_u$–$X^1\Sigma_g^+$), Ballik–Ramsay ($b^3\Sigma_g^-$–$a^3\Pi_u$), Swan ($d^3\Pi_g$–$a^3\Pi_u$), $d^3\Pi_g$–$c^3\Sigma_u^+$, $a^3\Pi_u$–$X^1\Sigma_g^+$, and $c^3\Sigma_u^+$–$X^1\Sigma_g^+$. Figure 1 represents these transitions and the electronic energy levels involved.

3.1. Calculation of the Energy Levels

The first step in the model is to compute numerical values for the molecular energy levels. These values were computed by using standard formulae with the constants given in Table I.

In the triplet system, each electronic state is split into three substates. For the $a^3\Pi_u$ state, the formulae used to compute the $F(J)$ values for the different substates ($F_1(J)$, $F_2(J)$, and $F_3(J)$) are given by Phillips (1968). These formulae use different constants for even and odd J values to account for lambda doubling. The T_e value given in Table I comes from Amiot *et al.* (1979), and the other constants come from Prasad and Bernath (1994).

For the $b^3\Sigma_g^-$ state, the rotational energies ($F_1(N)$, $F_2(N)$, and $F_3(N)$) were computed using the formulae of Ballik and

TABLE I
C_2 Constants Used to Calculate the Energy Levels (Expressed in cm^{-1})

State	$X^1\Sigma_g^+$	$a^3\Pi_u$	$b^3\Sigma_g^-$	$A^1\Pi_u$	$c^3\Sigma_u^+$	$d^3\Pi_g$
T_e	0	718.3181	6435.736	8391.643	9227.4	20024.5781
ω_e	1855.754	1641.32959	1470.415	1608.229	2040.5	
$\omega_e x_e$	14.136	11.651954	11.1549	12.089	14.1	
$\omega_e y_e$		$-1.6947 \cdot 10^{-3}$	$1.391 \cdot 10^{-2}$	-0.6		
B_e	1.820101		1.4986431	1.616560	1.88	
$\alpha_e\,(10^{-3})$	18.190		16.3121	16.953		
γ_e			$-4.61 \cdot 10^{-6}$	$-4.07 \cdot 10^{-5}$		
$D_e\,(10^{-6})$	6.9396		6.1958	6.4895		
$\beta_e\,(10^{-9})$	+66.9		-6.62	-27.4		
β_e'			$4.78 \cdot 10^{-10}$			

Ramsay (1963a). However, the higher-order spin-splitting terms in the constant γ and the cubic rotational constant H_v were neglected. The constants given in Table I are from Amiot *et al.* (1979).

For the $c^3\Sigma_u^+$ state, the constants given in Table I are from Chauville *et al.* (1977). Since the energy values for this state are very approximate, we used $F_1(N) = F_2(N) = F_3(N) = B_e N(N+1)$.

For the $d^3\Pi_g$ state, the constants are taken from Phillips (1968). The G(v) values were taken directly from the same paper. The $F(J)$ values were calculated with formulae similar to those used for the $a^3\Pi_u$ state.

The data given in Table I for the $X^1\Sigma_g^-$ and $A^1\Pi_u$ states are from Chauville *et al.* (1977). For the $A^1\Pi_u$ state, the energy difference due to lambda doubling was accounted for by applying a correction to the $F(J)$ values for even J such that $F'(J) = F(J) - q\,J(J+1)$ with $q = -1.954.10^{-4}$ cm^{-1} (Chauville *et al.* 1977). This correction is explained by Ballik and Ramsay (1963b).

It is important to note that T_e for the $a^3\Pi_u$ state, a key parameter for computing wavelengths in the $X^1\Sigma_g^+$–$a^3\Pi_u$ band, is an inferred value. The value was inferred from perturbations of $b^3\Sigma_g^-$ rotational energy levels by the $X^1\Sigma_g^+$ state. Ballik and Ramsay (1963a) studied these rotational perturbations for $v = 0$, 1, and 2 of the $b^3\Sigma_g^-$ state and found $T_e = 716.24$ cm^{-1} for the $a^3\Pi_u$ state. A more recent study (Amiot *et al.* 1979), including $v = 0$, 1, 2, 5, and 6, led to the T_e value given in Table I (i.e., 718.3181 cm^{-1}). The small difference in these two independent results implies that T_e is reasonably well determined.

The solar flux values used in the model are taken from NSO/Kitt Peak FTS data for the 2960 to 13000 Å range (Kurucz *et al.* 1984). These data are available online from NSF/NOAO. We have averaged the fluxes in 1-Å bins. Solar flux values from 13000 Å to 1 mm, with a stronger smoothing, are taken from Thekaekara (1974).

The model takes into account the heliocentric velocity of the comet by Doppler shifting the solar flux appropriately. However, given the smoothing of the model spectrum (1 Å), this correction is not accurate enough to accommodate the Greenstein effect for the Swan bands. This is because the energy values were computed using formulae, i.e., the wavelengths are not accurate enough to use a high-resolution solar spectrum. This is acceptable if one compares observational data with synthetic medium-resolution spectra as a whole, i.e., if the consequences of the Greenstein effect on a few lines are averaged over the hundreds of lines responsible for the observed spectrum.

3.2. Probability of Transitions

The band transition probabilities $A_{v'v''}$ were taken from Gredel *et al.* (1989) for the Swan system, from Chabalowski and Peyerimhoff (1983) for the Ballik–Ramsay system, and from Van Dishoeck (1983) for the Phillips system. For this last system, we preferred to normalize the $A_{v'v''}$ values using the oscillator strength $f_{00} = 2.0 \times 10^{-3}$.

For the $d^3\Pi_g$–$c^3\Sigma_u^+$ transition, we considered a constant ratio $A^{d-c}_{v'v''}/A^{d-a}_{v'v''}$. This ratio was a free parameter needed by the program. It was set equal to 0.1 for all calculations (see Section 4).

For the intercombination transitions, the band transition probabilities were computed by using

$$A_{v'v''} = 2.026\times10^{-6}[\Delta E^*]^3 \frac{|\sum D_e|^2}{N_{D_e}} q_{v'v''} \frac{c}{(2-\delta_{0,\Lambda'})(2S'+1)},$$

where ΔE^* is the wavenumber of the bandhead in cm^{-1}, $|\sum D_e|^2/N_{D_e}$ is the electronic transition moment in atomic units (a.u.), $q_{v'v''}$ is the Franck–Condon factor, and c is a summation factor (equal to 2 for the $a^3\Pi_u$–$X^1\Sigma_g^+$ transition and to 1 for the $c^3\Sigma_u^+$–$X^1\Sigma_g^+$ transition).

We computed the Franck–Condon factors for the $c^3\Sigma_u^+$–$X^1\Sigma_g^+$ and $a^3\Pi_u$–$X^1\Sigma_g^+$ transitions using a program based on an RKR method. Necessary molecular parameters were taken from Phillips (1968) for the $a^3\Pi_u$ state and from Chauville *et al.* (1977) for the $X^1\Sigma_g^+$ and $c^3\Sigma_u^+$ states. The internuclear distances used were taken from Huber and Herzberg (1977). The electronic transition moments $|D_{a-X}|^2$ and $|D_{c-X}|^2$ were considered as free parameters in the model (see Section 4).

The Hönl–London factors were taken from Le Bourlot (1987), for the Phillips and Swan transitions, and Kovacs (1969), for the other transitions. The Hönl–London factors $\mathcal{S}_{J'J''}(J)$ for the singlet and triplet transitions follow the summation rule

$$\sum_J \mathcal{S}_{J'J''}(J) = (2-\delta_{0,\Lambda'+\Lambda''})(2S+1)(2J+1).$$

The two intercombination transitions follow the summation rule:

$$\sum_J \mathcal{S}_{J'J''}(J) = c(2J+1),$$

where c is the summation factor mentioned above.

Singlet and triplet system line transition probabilities were computed from the band transition probabilities, $A_{v'v''}$, and the Hönl–London factors according to

$$A_{v'J'v''J''} = \frac{(2-\delta_{0,\Lambda'})}{(2-\delta_{0,\Lambda'+\Lambda''})} \frac{[\Delta E]^3}{[\Delta E^*]^3} A_{v'v''} \frac{\mathcal{S}_{J'J''}}{2J'+1},$$

where ΔE is the wavenumber of the line considered. For the intercombination transitions the following formula was used:

$$A_{v'J'v''J''} = \frac{(2-\delta_{0,\Lambda'})(2S'+1)}{c} \frac{[\Delta E]^3}{[\Delta E^*]^3} A_{v'v''} \frac{\mathcal{S}_{J'J''}}{2J'+1}.$$

The absorption rates $B_{v''J''v'J'}$ were computed from the $A_{v'J'v''J''}$ values. The stimulated emission was neglected because of its extreme weakness compared to spontaneous emission.

3.3. Method of Calculation

The matrix method described by Zucconi and Festou (1985) was used to compute the fluorescent equilibrium solution. The levels considered as ground states in considering this formalism are the $X^1\Sigma_g^+$, $a^3\Pi_u$, and $c^3\Sigma_u^+$ states. These states are characterized by relatively long lifetimes and internal transitions or absorption processes toward excited states. The excited states have much shorter lifetimes and have no internal transitions. They decay only toward the ground states.

The linear set of algebraic equations which has to be solved when using this method was computed by using an LU decompositon. This method simplifies the calculations by writing the matrix to invert as a product of a lower triangular (L) matrix and an upper triangular (U) matrix. The formalism given by Zucconi and Festou allows us to reduce the size of the matrix to invert to 2693 (i.e., the number of ground states − 1), for a total of 5652 energy levels.

Once the relative population levels are known for the ground states, it is easy to compute those of the excited states. To compute the relative population x_i of a level i belonging to the $d^3\Pi_g$ state we used the equality

$$\sum_{j=1}^{N_X} B_{ji}\rho_\nu x_j = \sum_{j=1}^{N_X} A_{ij}x_i,$$

where ρ_ν is the solar radiation density. This equation directly gives the x_i values for the $d^3\Pi_g$ state sublevels:

$$x_i = \frac{\sum_{j=1}^{N_X} B_{ji}\rho_\nu x_j}{\sum_{j=1}^{N_X} A_{ij}}.$$

These relative populations lead to the synthetic spectrum by using the line transition probabilities $A_{v'J'v''J''}$.

4. COMPARISON OF THE MODEL WITH THE OBSERVATIONS

The first step in comparing the observational data with the model was to select only the spectra corresponding to fluorescent equilibrium. An intensity ratio was displayed using all the spectra to identify the cometocentric distances for which fluorescent equilibrium is reached. The ratio computed was $I(\lambda = 5133$–5143 Å$)/I(\lambda = 5162$–5167 Å). It was chosen because its variation is sensitive only to the (0, 0) band rotational temperature. (The (1,1) bandhead is located at shorter wavelengths and this band is degraded to the blue.) A larger ratio indicates a higher rotational temperature. This is because shorter wavelengths correspond both to the lines of the R branch having low J-values ($J \simeq 10$) and to the lines of the P branch having high J-values ($J \simeq 40$) (see Rousselot *et al.* 1995, Fig. 3). The longer wavelengths correspond to the P branch and the bandhead (J-values inferior to about 20). Examination of this ratio versus cometocentric distance revealed that the lower rotational temperatures occur near the nucleus and increase with cometocentric distance out to about 60,000 km.

By using all the spectra obtained between 60,000 and 240,000 km, an average spectrum was obtained. This spectrum is representative of C_2 fluorescent equilibrium conditions at 3.03 AU from the Sun.

To simplify comparison of the observational data with the theoretical spectra, we considered a constant ratio $A^{d-c}_{v'v''}/A^{d-a}_{v'v''} = 0.1$. The electronic transition moments $|D_{a-X}|^2$ and $|D_{c-X}|^2$ were also considered equal.

Although this last assumption is probably not realistic, Gredel *et al.* (1989) note that the $c^3\Sigma_u^+$–$X^1\Sigma_g^+$ transition is only of secondary importance to the equilibrium populations because of the lesser importance of the $d^3\Pi_g$–$c^3\Sigma_u^+$ transition. Given the accuracy of the observational data, it would be difficult to distinguish the effects of different values of $|D_{c-X}|^2$ for a given intercombination transition moment $|D_{a-X}|^2$. However, it seems better to take into account the $c^3\Sigma_u^+$–$X^1\Sigma_g^+$ transition. Thus, a good way to test the value $|D_{a-X}|^2$ is to give a similar value to $|D_{c-X}|^2$. In addition to these general considerations, note that Gredel *et al.* (1989) used also a similar value for these two parameters (i.e., 3.5×10^{-6} a.u.).

Given the results previously obtained by other authors (A'Hearn and Feldman 1980, Lambert and Danks 1983, Krishna Swamy and O'Dell 1987, O'Dell *et al.* 1988, Gredel *et al.* 1989), this study focused on reasonable expected values of $|D_{a-X}|^2$, i.e., around 10^{-6} and 10^{-5} a.u.

Figure 2 shows the results obtained for four different values of $|D_{a-X}|^2$ and $|D_{c-X}|^2$: 10^{-6}, 5×10^{-6}, 10^{-5}, and 5×10^{-5} a.u. All the theoretical spectra are adjusted in intensity, to match the experimental spectra and facilitate comparison of the rotational structure.

To more objectively compare the quality of the fit obtained for each synthetic spectrum, a relative χ^2 test was performed. For each pair of spectra (observed/synthetic) the following parameter was computed:

$$\chi^2 = \sum_{i=1}^{N} \frac{\left(I_{\mathrm{obs}_i} - I_{\mathrm{syn}_i}\right)^2}{I_{\mathrm{obs}_i}}.$$

In this formula I_{obs_i}, is the observed intensity of the ith pixel, I_{syn_i}, is the intensity of the ith pixel of the synthetic spectrum, and N is the total number of pixels in the spectrum. The uncertainty assumed in this formulation is the square root of the intensity. A lower number indicates a better fit.

The χ^2 computed, when normalized to 1 for the smallest value, were, respectively, 2.95, 1, 1.13, and 3.13 for $|D_{a-X}|^2 = |D_{c-X}|^2 = 10^{-6}$, 5.10^{-6}, 10^{-5}, and 5.10^{-5}. Our conclusion is, then, that $5 \times 10^{-6} \leq |D_{a-X}|^2 \leq 10^{-5}$ a.u. With the accuracy of both the model and the observational data, it seems difficult to be more precise in the estimation of these values.

This range of $|D_{a-X}|^2$ values is in agreement with the results obtained by previous studies. One of the first attempts to derive a quantitative value for this parameter was done by

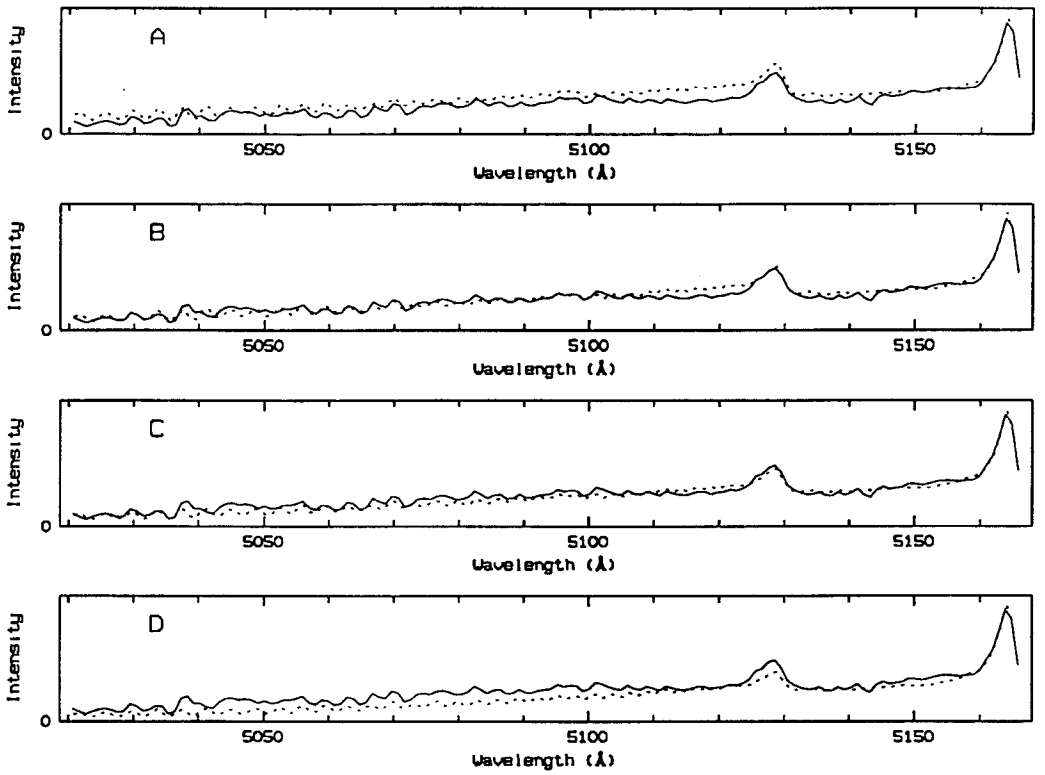

FIG. 2. Comparison of the average Hale-Bopp spectrum obtained on October 12, 1997, with theoretical results. A: $|D_{a-X}|^2 = |D_{c-X}|^2 = 10^{-6}$ a.u. B: $|D_{a-X}|^2 = |D_{c-X}|^2 = 5 \times 10^{-6}$ a.u. C: $|D_{a-X}|^2 = |D_{c-X}|^2 = 10^{-5}$ a.u. D: $|D_{a-X}|^2 = |D_{c-X}|^2 = 5 \times 10^{-5}$ a.u.

A'Hearn and Feldman (1980). Their study led to a value varying from about 10^{-5} to 2×10^{-5} a.u. This study was based on the measurement of the flux ratio of the Mulliken and Swan system $\Delta v = 0$. However, the Mulliken and Phillips system f-values used were improved after their study and could affect their conclusions. Lambert and Danks (1983) tried to estimate $|D_{a-X}|^2$ both theoretically (they found about 10^{-7} a.u.) and from observational data (they found about 5×10^{-5} a.u.). They suggested that the $c^3\Sigma_u^+ - X^1\Sigma_g^+$ transition, not taken into account in their study, could explain the difference between the two results. Krishna Swamy and O'Dell (1987) published an estimated value of about 10^{-5} a.u. using a model based on vibrational levels (including the $c^3\Sigma_u^+ - X^1\Sigma_g^+$ transition) compared to the Swan band sequence flux ratio. O'Dell *et al.* (1988) used a similar method to find a value of 2.5×10^{-6} a.u., using spectra of comet Halley. Gredel *et al.* (1989), as already mentioned, used a value of $|D_{a-X}|^2$ equal to $|D_{c-X}|^2$ and to 3.5×10^{-6} a.u.

For $|D_{a-X}|^2 = |D_{c-X}|^2 = 5 \times 10^{-6}$ it is interesting to examine the distribution of the relative population levels obtained from the model. These relative populations are shown in Fig. 3. They are shown for the $d^3\Pi_g v = 0$ vibrational level for each of the F_1, F_2, and F_3 sublevels.

The solid lines in Fig. 3 for each of the F_1, F_2, and F_3 sublevels correspond to the best fit obtained by assuming that the relative populations are Boltzmann distributions. For this fit only the levels with $29 < J < 90$ were taken into account. Clearly

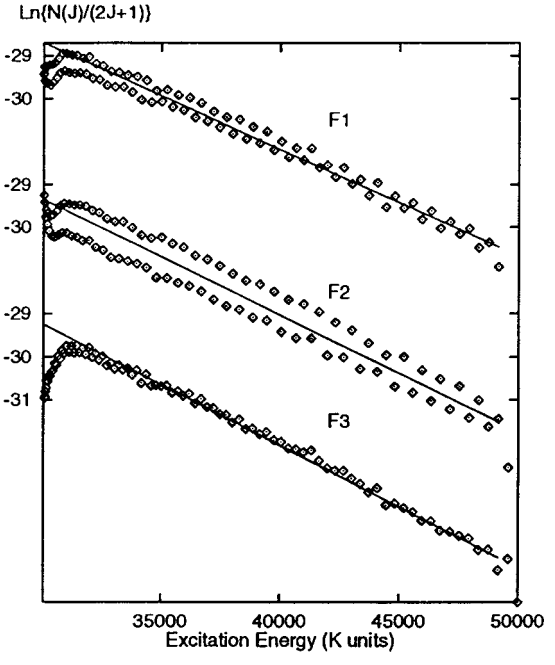

FIG. 3. Relative populations obtained for the $d^3\Pi_g v = 0$ rotational levels (with $R = 3.03$ AU). The three sublevels F_1, F_2, and F_3 are represented. The lines represent the best fits obtained for a Boltzmann distribution computed for $J \geq 30$. For F_1, the best fit corresponds to 4013 K, for F_2 to 3710 K, and for F_3 to 3529 K.

TABLE II

Average Rotational and Vibrational Temperatures Given by the Model for the $d^3\Pi_g$ State (and $v = 0$ for the Rotational Temperature)

R (AU)	T_{rot}	T_{vib}
0.94	4670	5211
3.03	3750	3903

Note. $|D_{a-X}|^2 = |D_{c-X}|^2 = 5 \times 10^{-6}$ a.u. The values given for $R = 0.94$ AU are given for a comparison with the situation around the perihelion passage of Comet Hale-Bopp.

the sublevels corresponding to smaller J values do not follow a Boltzmann distribution. Table II shows the average rotational temperatures obtained using this method and the vibrational temperatures for $|D_{a-X}|^2 = 5 \times 10^{-6}$ a.u.

Note that there is an odd–even effect in the population distribution among rotational levels (Fig. 3). We have no clear explanation concerning this effect; however, it had also been seen by Gredel *et al.* (1989). They interpreted this result as being due to the differences in the line intensity factors for the three intercombination sub-transitions, treated separately for each of the three spin components of the triplet states.

5. CONCLUSION

We have shown that it is possible to satisfactorily model spectra of the C_2 Swan band $\Delta v = 0$ sequence obtained far from the nucleus and at a large heliocentric distance for Comet Hale-Bopp. This model, adapted to medium-resolution spectra, can also explain the observed sequence on the whole. The observational data can be modeled with $5 \times 10^{-6} \leq |D_{a-X}|^2 \leq 10^{-5}$ a.u. given the following model assumptions: Phillips oscillator strength $f_{00} = 2.0 \times 10^{-3}$, ratio $A^{d-c}_{v'v''}/A^{d-a}_{v'v''} = 0.1$, and $|D_{a-X}|^2 = |D_{c-X}|^2$.

The uncertainties involved in this type of modeling are significant, especially in the accuracy of the inputs (e.g., the $A_{v'v''}$ values for the $d^3\Pi_g$–$c^3\Sigma_u^+$ transition or the $|D_{c-X}|^2$ value). Because of the limitations of our approach, improvements in the accuracy should be obtained by other methods, e.g., laboratory experiments or purely theoretical calculations. The results obtained by using cometary spectra can, however, be useful to test the results obtained through other methods.

REFERENCES

A'Hearn, M. F., and P. D. Feldman 1980. Carbon in Comet Bradfield 1979I. *Astrophys. J.* **242**, L187–L190.

Amiot, C., J. Chauville, and J. P. Maillard 1979. New analysis of the C_2 Ballik–Ramsay system from flame emission spectra. *J. Mol. Spectrosc.* **75**, 19–40.

Ballik, E. A., and D. A. Ramsay 1963a. The $A'^3\Sigma_g^- - X'^3\Pi_u$ band system of the C_2 molecule. *Astrophys. J.* **137**, 61–83.

Ballik, E. A., and D. A. Ramsay 1963b. An extension of the Phillips system of C_2 and a survey of C_2 states. *Astrophys. J.* **137**, 84–101.

Chabalowski, C. F., and S. D. Peyerimhoff 1983. The Ballik–Ramsay, Mulliken, Deslandres–d'Azambuja, and Phillips system in C_2: A theoretical study of their electronic transition moments. *Chem. Phys.* **81**, 57–72.

Chauville, J., and J. P. Maillard 1977. The infrared part of the C_2 Phillips system (2.3–0.9 μm). *J. Mol. Spectrosc.* **68**, 399–411.

Gredel, R., E. F. Van Dishoeck, and J. H. Black 1989. Fluorescent vibration-rotation excitation of cometary C_2. *Astrophys. J.* **338**, 1047–1070.

Huber, K. P., and G. Herzberg 1977. *Constants of Diatomic Molecules*. Van Nostrand–Reinhold, NewYork.

Kovacs, J. 1969. *Rotational Structure in the Spectra of Diatomic Molecules*. Hilger, London.

Krishna Swamy, K. S., and C. R. O'Dell 1987. Statistical equilibrium in cometary C_2. A 10 level model including singlet–triplet transitions. *Astrophys. J.* **317**, 543–550.

Kurucz, L., I. Furenlid, J. Brault, and L. Testerman 1984. Solar flux atlas from 296 to 1300 nm. In *National Solar Observatory Atlas Number 1*.

Laffont, C., P. Rousselot, J. Clairemidi, and G. Moreels 1998. Condensations and diffuse sources of C_2 in Comet Hyakutake C/1996 B2. *Planet. Space Sci.* **46**, 585–601.

Lambert, D. L., and A. C. Danks 1983. High-resolution spectra of C_2 Swan bands from Comet West 1976 VI. *Astrophys. J.* **268**, 428–446.

Le Bourlot, J. 1987. Calcul de probabilités de transitions d'intercombinaison entre les états $X^1\Sigma_g^+$ et $a^3\Pi_u$ de C_2. Application à l'équilibre de C_2 dans les nuages interstellaires diffus. Ph.D. thesis, University of Paris VII.

Le Bourlot, J., and E. Roueff 1986. Intercombination transitions between levels $X^1\Sigma_g^+$ and $a^3\Pi_u$ in C_2. *J. Mol. Spectrosc.* **120**, 157–168.

O'Dell, C. R., R. R. Robinson, K. S. Krishna Swamy, P. J. McCarthy, and H. Spinrad 1988. C_2 in Comet Halley: Evidence for its being third generation and resolution of the vibrational population discrepancy. *Astrophys. J.* **334**, 476–488.

Phillips, J. G. 1968. Perturbations in the Swan system of the C_2 molecule. *J. Mol. Spectrosc.* **28**, 233–242.

Prasad, C. V. V., and P. F. Bernath 1994. Fourier transform spectroscopy of the Swan ($d^3\Pi_g$–$a^3\Pi_u$) system of the jet-cooled C_2 molecule. *Astrophys. J.* **426**, 812–821.

Rousselot, P., J. Clairemidi, and G. Moreels 1994. Evolution of the C_2 spectrum in Halley's inner coma: Evidence for a diffuse source. *Astron. Astrophys.* **286**, 645–653.

Rousselot, P., C. Laffont, G. Moreels, and J. Clairemidi 1998. An attempt to detect the C_2 intercombination transition lines in Comet Hale-Bopp. *Astron. Astrophys.* **335**, 765–768.

Rousselot, P., G. Moreels, J. Clairemidi, B. Goidet-Devel, and H. Boehnhardt 1995. Evolution of the C_2 spectrum in comets P/Schaumasse and P/Tempel 2. *Icarus* **114**, 341–347.

Thekaekara, M. P. 1974. Extraterrestrial solar spectrum, 3000–6100 Å at 1 Å intervals. *Appl. Optics* **13**(3), 518–522.

Van Dishoeck, E. F. 1983. Oscillator strengths and lifetimes of the C_2 $A^1\Pi_u \rightarrow X^1\Sigma_g^+$ Phillips system. *Chem. Phys.* **77**, 277–286.

Zucconi, J. M., and M. C. Festou 1985. The fluorescence spectrum of the CN radical in comets. *Astron. Astrophys.* **150**, 180–191.